

H I and optical observations of dwarf galaxies

L. Staveley-Smith,¹★ R. D. Davies¹ and T. D. Kinman²

¹University of Manchester, Nuffield Radio Astronomy Laboratories, Jodrell Bank, Macclesfield, Cheshire SK11 9DL

²National Optical Astronomy Observatories,† PO Box 26732, Tucson, Arizona 85726, USA

Accepted 1992 March 12. Received 1992 March 12; in original form 1991 December 11

SUMMARY

H I observations have been made with the 76-m Lovell Telescope of 36 galaxies of the blue compact and the low surface brightness type, of which 23 are true dwarfs ($M_B \geq -16$ mag) and 31 have optical diameters less than 10 kpc. Photoelectric photometry from the Kitt Peak 2.1-m telescope reveals systematic errors in previous studies. The observations confirm the relative hydrogen richness of dwarf galaxies and indicate an increase in gas richness with decreasing luminosity. The distribution of intrinsic dwarf galaxy shapes is derived and applied to the statistical calculation of dwarf galaxy total masses, taking into account support by internal pressure. The contribution of dwarf galaxies to the total luminosity density in the nearby Universe is ~ 10 per cent and their H I contribution is ~ 30 per cent.

Key words: galaxies: compact – galaxies: fundamental parameters – galaxies: interstellar matter – galaxies: photometry – radio lines: atomic.

1 INTRODUCTION

Dwarf galaxies are by far the most numerous objects in the extragalactic Universe. Some 80 per cent of the known Local Group galaxies are dwarfs, and the space density of dwarfs may be about 40 times that of bright galaxies (see below). In this paper we use the commonly accepted distance-dependent luminosity definition that any galaxy fainter than $M_B = -16$ mag is a dwarf (Tammann 1980). However, some ‘blue compact objects’ which have similar H I contents to those of dwarfs with low surface brightness (LSBs) are often classified as dwarfs because of their small linear sizes ($\lesssim 5$ kpc), and may be brighter than this -16 -mag limit. We describe here an H I and optical study of a selected sample of dwarf galaxies.

Three types of dwarf galaxy have been identified: their properties are described below.

(i) Dwarf LSB galaxies include both irregular (Im) galaxies and the more regular (Sm) galaxies (Longmore *et al.* 1982; Reaves 1983; Binggeli, Sandage & Tarenghi 1984). They all contain large amounts of H I, often have small knots (OB associations), and have blue colours ($B - V \approx 0.5$ mag) indicating a significant level of recent star formation or the presence of old metal-deficient stars. LSB galaxies in the

field have been well studied in H I by Fisher & Tully (1975) who observed the van den Bergh DDO sample of 243 galaxies, by Thuan & Seitzer (1979a) who detected H I in 145 galaxies classified as dwarf in the Uppsala General Catalogue (UGC) of galaxies (Nilson 1973), and by Schneider *et al.* (1990) who studied a more comprehensive sample of late-type UGC galaxies. Many of the objects included in these surveys turn out not to be dwarf galaxies on our definition. Hoffman, Helou & Salpeter (1988) have studied the H I emission from 293 so-called dwarfs in the Virgo cluster; the detection rate fell to 20 per cent for the true dwarfs in the sample which still had a high ratio of $M_H/L_B (\sim 1.0)$. The true dwarfs in the NGC 1023 group also have $M_H/L_B \sim 1.0$ (Davies & Kinman 1984).

(ii) Dwarf elliptical galaxies are found predominantly in groups and clusters. They were studied as a class in the Virgo cluster by Reaves (1983). The atlas of dwarfs in the Virgo cluster published by Sandage & Binggeli (1984) classifies 80 per cent as dwarf ellipticals which form a gradual progression in properties from the larger ellipticals. As is the case for the larger ellipticals, only about 10 per cent of the dwarfs contain detectable H I (Kraan-Korteweg & Tammann 1979; Huchtmeier 1980). We do not consider them further in the present study.

(iii) Blue compact galaxies (BCGs) have small dimensions and amorphous shapes with no spiral structure. They contain giant H II regions surrounding O and B stars within a massive H I reservoir. Searle & Sargent (1972) proposed that BCGs were actually LSB galaxies in which a sudden burst of star formation had taken place. In the most metal-poor BCGs

★ Present address: Australia Telescope National Facility, CSIRO, PO Box 76, Epping, NSW 2121, Australia.

† Operated by the Association of Universities for Research on Astronomy, Inc., under contract with the National Science Foundation.

there have been only a few such bursts within the age of the Universe. Sandage & Binggeli (1984) classify BCGs as an extension from spiral through Im to BCG, which is a sequence going from galaxies supported by rotation to those supported largely by random motion or even being disrupted by supernova and starburst-type phenomena. A majority of the 50 BCGs studied by Loose & Thuan (1985) and Kunth, Maurogordato & Vigroux (1988) have extended structure indicative of an underlying LSB galaxy. The dynamical and chemical evolution of low-mass BCGs will be heavily modified by supernova explosions (De Young & Gallagher 1990).

The present paper describes H I and optical observations of 36 low-luminosity LSB galaxies and BCGs which are being used to build up a data base to compare the integrated properties of these two classes of galaxy. Objects were selected from the literature, mainly from the lists of Haro for the BCGs and the UGC for the LSBs. The sample studied is in no way complete, but is representative of the population. Section 2 describes the H I observations and optical photometry. Section 3 describes the derived H I and optical parameters of the galaxies and discusses overall trends. Section 4 discusses luminosity functions and starbursts. We assume $H_0 = 75 \text{ km s}^{-1} \text{ Mpc}^{-1}$.

2 OBSERVATIONS

All the H I observations presented here were made with the 76-m Lovell Telescope at Jodrell Bank. Most observations were made with parametric amplifier receivers with noise temperatures of approximately 80 K; weaker galaxies were observed with 40-K cooled FET amplifiers. Two modes of observation were employed for the dwarf galaxies.

(i) Frequency-switching the local oscillator during successive 100-s integrations and subtracting alternate spectra. The frequency switch was such as to keep the emission from the galaxy within the bandpass in each spectrum.

(ii) Beam-switching the telescope by tracking off-source 8 min higher in right ascension during successive 500-s integrations, thereby producing a flatter baseline but requiring twice the observing time for the same sensitivity.

The off-line reduction of the data consisted of removing low-order polynomials from the spectra to obtain flat baselines, and the derivation of velocity and flux parameters from the line profiles of each galaxy. The H I spectra of the 36 detected galaxies are shown in Fig. 1. The velocity resolution is 7 km s^{-1} for all spectra except 1457–00, NGC 5811, 2228–00 (14 km s^{-1}) and Mkn 429 (25 km s^{-1}). These H I observations form an internally consistent data set; the flux scale agrees closely with that of Fisher & Tully (1981) with which there are 10 galaxies in common.

Multi-aperture photoelectric B magnitudes were obtained of 22 galaxies at the 2.1-m telescope at Kitt Peak. The magnitudes were derived in the B_T system of de Vaucouleurs; they have an estimated error of 0.1 mag. 11 other photoelectric magnitudes were taken from RC2 (de Vaucouleurs, de Vaucouleurs & Corwin 1976), Kinman *et al.* (1977), Kinman & Davidson (1981) and Kinman & Hintzen (1981). One further magnitude was from Kinman & Conklin (private communication). The remaining two galaxies do not have

photoelectric magnitudes. Approximate magnitudes are given in Table 1 using, for one, the eye estimate of Thuan & Seitzer (1979a) corrected to the B_T system ($\sigma=0.5 \text{ mag}$), and, for the other, the Zwicky magnitude corrected to the B_T system using the formula given by Auman, Hickson & Fahlman (1982) ($\sigma=0.3 \text{ mag}$). The two non-photoelectric measurements are not included in the discussion or any figures.

29 of the 36 galaxies have published angular diameters and axial ratios in UGC, RC2, Kinman & Davidson (1981) and Kinman & Hintzen (1981). Data for another two galaxies were given by Kinman & Conklin (private communication). We derived dimensions for four galaxies from calibrated CCD images and for one galaxy from Palomar Sky Survey prints using the UGC scale.

For consistency with previous authors we use the Holmberg (1958) system for estimating diameters and axial ratios, based on a limiting isophote of $26.5 \text{ mag arcsec}^{-2}$ in the blue. For the 22 galaxies in our sample without Holmberg dimensions, we have used calibration factors based on a direct comparison between Holmberg diameters and those given by RC2 and UGC for late-type IrrI galaxies. We find the average ratio of Holmberg-to-RC2 diameters to be 1.65 ± 0.07 for 21 galaxies; for Holmberg-to-UGC diameters the ratio is 1.38 ± 0.08 for 18 galaxies. To obtain the axial ratios on the Holmberg scale, we use the conversion formulae given by Fisher & Tully (1981). Because of the heterogeneous nature of the diameter data, there are likely to be significant errors in the values listed in Table 1.

2.1 Observed properties

Of the 36 galaxies in the sample, 21 are LSB galaxies and 15 are BCGs (these are sometimes classified as ‘peculiar’ galaxies). Table 1 lists the observed H I and optical parameters of the programme galaxies.

The column entries in Table 1 are given below.

- (1) Galaxy identification.
- (2) Right ascension and declination in 1950 coordinates.
- (3) *Line 1*: Holmberg diameter a_H in arcmin, at the $26.5 \text{ mag arcsec}^{-2}$ blue isophote.
Line 2: Holmberg axial ratio, p_H .
- (4) Source of the uncorrected diameter data according to the coding at the foot of the table.
- (5) Heliocentric velocity, V_H in km s^{-1} corrected to the optical convention $v = c\Delta\lambda/\lambda_0$, together with the estimated error. This is the velocity mid-way between the half-power points measured separately on each side of the spectrum.
- (6) Velocity width W_{20} of the H I profile in km s^{-1} at the 20 per cent level together with error. Where the profile is asymmetric (e.g. UGC 9427 = NGC 5692 = Akn 454), the difference of the fifth power points of each end of the spectrum was used.
- (7) Velocity width W_{50} at the 50 per cent level and error.
- (8) Flux density integral, FI , in Jy km s^{-1} uncorrected for beam dilution. A minimum error of 10 per cent is assigned to account for baseline and flux scale uncertainties.
- (9) Integrated blue magnitude, B_T , in the RC2 system.
- (10) Source of the magnitude data according to the coding at the foot of the table.
- (11) Description of the galaxy. (*) signifies a BCG.

Table 1. Observed galaxy properties.

(1)	(2)	(3)	(4)	(5)	(6)	(7)	(8)	(9)	(10)	(11)
GALAXY	R.A. DEC (1950)	$a_H(^{\circ})$ p_H	SOURCE	V_H σ	W_{20} σ	W_{50} σ	FI σ	B_T σ	SOURCE	Description
				km s ⁻¹		Jy km s ⁻¹				
0049-01	00 49 26 -01 56.6	0.43 0.53	KH	1914 10	76 20	53 16	0.8 0.2	17.33	KH	UV-excess galaxy (*)
0049-00	00 49 26 -00 45.5	1.0 0.42	KH	1622 4	196 12	173 8	15.8 2.7	15.25	KH	UV-excess galaxy (*)
UGC 695	01 05 12 +00 47.8	1.8 0.86	UGC	630 4	91 12	55 6	3.4 0.5	15.1	SDK	Peculiar
DDO 26	02 31 30 +29 32.	3.5 0.58	RC2	1023 4	89 12	59 8	14.0 1.6	15.20	RC2	Dwarf Irregular
Mkn 600	02 48 28 +04 14.8	0.85 0.66	KD	1016 6	115 16	87 12	6.8 1.3	15.42	KD	UV continuum (*)
UGC 2684	03 17 34 +17 06.9	2.8 0.55	UGC	348 4	91 12	80 8	8.4 1.5	16.5	SDK	Dwarf ?
UGC 3817	07 19 07 +45 12.0	2.8 0.55	UGC	438 3	56 6	40 4	7.9 2.5	15.8	SDK	Dwarf
DDO 47	07 39 03 +16 55.1	7.7 0.83	RC2	272 2	87 6	70 4	47. 7.	13.54	RC2	Dwarf Irregular
UGC 4483	08 32 14 +69 57.2	1.9 0.55	UGC	155 2	56 6	36 4	12.3 2.8	15.0	SDK	Dwarf-comp superimp
UGC 4824	09 08 00 +51 28.	3.4 0.31	UGC	551 8	52 14	39 12	1.1 0.4	14.3	ZAHF	SAd
1 Zw 18	09 30 30 +55 27.7	0.6 0.4	KD	754 6	82 16	57 12	3.4 0.6	16.17	KD	Blue Compact (*)
UGC 6248	11 10 16 +10 28.4	2.2 0.83	UGC	1289 4	38 12	25 8	1.6 0.6	16.0	SDK	Dwarf Irregular
UGC 6881	11 52 27 +20 20.0	2.2 0.49	UGC	601 8	118 18	90 14	3.2 0.4	15.8	SDK	Dwarf
UGC 7207	12 09 54 +37 17.4	4.1 0.57	RC2	1051 6	87 14	74 12	5.3 1.2	14.5	TS	Dwarf Irregular
UGC 7298	12 14 01 +52 30.3	1.7 0.62	UGC	168 3	49 8	27 6	5.3 0.9	15.8	SDK	Dwarf
RMB 56	12 16 42 +14 09.6	0.52 0.85	KC	-235 8	102 20	82 16	1.9 0.2	16.05	KRTFP	Blue Compact (*)
1 Zw 36	12 23 52 +48 46.2	1.4 0.90	RC2	282 3	70 8	49 6	7.6 0.7	14.5	RC2	Blue Compact (*)
UGC 7605	12 26 10 +35 59.4	2.2 0.72	UGC	309 5	58 16	30 10	5.3 1.8	14.5	SDK	Dwarf Irregular
RMB 132	12 28 18 +12 19.	0.38 0.73	KD	1263 8	115 20	84 16	1.4 0.3	17.06	KD	Blue Compact (*)
UGC 7903	12 41 28 +54 13.8	1.4 1.0	UGC	443 4	85 12	69 8	6.8 0.7	16.0	SDK	Dwarf
UGC 8055	12 53 31 +04 04.9	1.4 0.82	UGC	616 4	105 12	94 8	7.4 0.9	15.6	SDK	Dwarf Irregular
UGC 8215	13 05 50 +47 05.4	1.4 0.82	UGC	216 4	45 8	29 6	3.8 0.9	15.9	SDK	Dwarf Irregular
UGC 8276	13 09 34 +05 44.2	1.4 0.55	UGC	908 6	91 16	75 12	2.7 0.5	16.1	SDK	Dwarf
Mkn 450	13 12 29 +35 08.6	1.5 0.63	KD	861 5	89 13	70 10	3.3 0.8	14.50	KD	UV-continuum (*)
UGC 9427	14 35 48 +03 37.5	1.4 0.68	SDK	1581 6	198 20	150 12	2.9 0.2	13.6	SDK	Emission line galaxy (*)
Mkn 429	14 43 49 +35 07.8	0.7 0.95	KC	1415 20	225 40	168 30	2.8 1.0	14.7	KC	UV-continuum (*)
1457-00	14 57 24 -00 53.6	0.37 1.0	SDK	1901 6	95 13	84 8	1.1 0.3	15.7	SDK	Emission line galaxy(*)
NGC 5811	14 57 54 +01 49.3	1.3 0.81	SDK	1532 6	91 16	74 12	1.3 0.3	14.6	SDK	Emission line galaxy (*)
UGC 9661	14 59 30 +02 02.2	1.7 0.78	SDK	1241 6	115 16	91 12	1.4 0.8	14.3	SDK	Emission line SBdm (*)
1501+00	15 01 24 +00 37.6	0.78 0.72	SDK	1593 4	57 8	37 6	1.1 0.4	16.3	SDK	Emission line galaxy (*)
UGC 10669	17 00 53 +70 21.6	1.9 1.0	UGC	443 3	54 8	29 6	2.6 0.6	16.4	SDK	Dwarf
2228-00	22 28 00 -00 23.	0.28 0.45	KD	1591 20	123 30	82 30	0.6 0.2	17.72	KD	Blue Compact (*)

Table 1 - continued

(1)	(2)	(3)	(4)	(5)	(6)	(7)	(8)	(9)	(10)	(11)
GALAXY	R.A. DEC	$a_H(^{\circ})$ p_H	SOURCE	V_H σ	W_{20} σ	W_{50} σ	FI σ	B_T σ	SOURCE	Description
					km s ⁻¹			Jy km s ⁻¹		
DDO 214	22 33 59 -03 09.9	3.5 0.87	RC2	1690 4	129 12	110 8	18.4 3.4	13.6	SDK	SA(s)m
UGC 12151	22 39 00 +00 08.3	4.1 0.7	UGC	1759 6	200 20	161 12	18.4 3.4	14.5	SDK	Dwarf
UGC 12178	22 42 36 +06 10.	5.2 0.58	RC2	1928 4	227 12	218 8	23.1 3.6	13.3	SDK	SAB(s)dm
UGC 12894	23 57 48 +39 12.9	1.4 1.0	UGC	334 3	37 8	27 6	4.5 0.9	16.5	SDK	Dwarf irregular

Notes. A bracketed asterisk (*) in the last column signifies a galaxy classified as blue compact for the purposes of this paper. The sources of the diameter and magnitude data are: SDK, this paper; KC, Kinman & Conklin (private communication); KD, Kinman & Davidson (1981); KH, Kinman & Hintzen (1981); KRTFP, Kinman *et al.* (1977); UGC, Nilson (1973); RC2, Second Reference Catalogue (de Vaucouleurs, de Vaucouleurs & Corwin 1976); TS, Thuan & Seitzer (1979a); ZAHF, Zwicky magnitude corrected according to Auman, Hickson & Fahlman (1982).

2.2 Derived properties

Table 2 lists the derived properties for those galaxies which we detected in H I. The column entries are as follows.

- (1) Galaxy identification.
- (2) Galactic longitude, l , and latitude, b .
- (3) Velocity with respect to the Local Group centroid, V_0 . This is the heliocentric systemic velocity, V_H , corrected for the rotation of our Galaxy and its motion in the Local Group using the IAU convention

$$V_0 = V_H + 300 \sin l \cos b \text{ (km s}^{-1}\text{)}.$$

- (4) Distance D , in Mpc assuming $H_0 = 75 \text{ km s}^{-1} \text{ Mpc}^{-1}$ unless listed at the foot of the table.
- (5) Linear Holmberg diameter in kpc.
- (6) Corrected hydrogen flux (F_c) in units of $10^6 M_{\odot} \text{ Mpc}^{-2}$ and beam correction factor (f_c), where $F_c = 2.36 \times 10^5 f_c FI$. f_c is defined in Section 3.2.

The following properties are statistically derived and their derivation is explained more fully in Section 3.

- (7) *Line 1*: intrinsic axial ratio, q_0 , assuming galaxies to be oblate spheroids. Method of calculation is given in Appendix A.

Line 2: inclination, in degrees, from face-on calculated using equation (A7).

- (8) *Line 1*: line-of-sight velocity dispersion (km s^{-1}), assuming it to be isotropic and responsible for the intrinsic shape of the galaxy. See Appendix A.

Line 2: estimated rotation velocity (km s^{-1}) de-projected. See Appendix A.

- (9) *Line 1*: the mass of the galaxy within the Holmberg radius in units of $10^8 M_{\odot}$.

Line 2: the mass of the galaxy as above (in units of $10^8 M_{\odot}$) with the alternative hypothesis that velocity dispersion is constant at 10 km s^{-1} .

- (10) *Line 1*: absolute blue magnitude, M_B .

Line 2: correction used for the absorption within our own Galaxy is $\Delta M_B = -0.2 \text{ cosec } b \text{ mag}$.

No correction has been applied for possible inclination-dependent internal reddening, as this is small for the sample of inflated galaxies studied here. Holmberg (1958), for example, finds no such effect in his sample of 10 Irr I galaxies.

(11) Logarithm of the absolute luminosity, L_B , in solar luminosities assuming $M_B(\text{Sun}) = 5.41$ (Lang 1974).

(12) Logarithm of the hydrogen mass, M_H , in solar masses, where $M_H = F_c D^2$.

(13) Logarithm of the total mass, M_T , in solar masses from column 8, line 1.

3 THE INTEGRATED PROPERTIES OF DWARF GALAXIES

3.1 Blue luminosity

Accurate blue luminosities are central to our discussion of the H I properties of dwarf galaxies. For the majority of our galaxies we have reliable photometry obtained either by ourselves or from published sources. In an early paper on the H I properties of LSB galaxies, Thuan & Seitzer (1979a) estimated magnitudes by eye from the Palomar Observatory Sky Survey prints and calibrated them on the B_T scale. We have new optical observations for 13 galaxies common between our lists; their magnitudes are systematically too bright by about 0.5 mag. The systematic overestimate in the brightness of LSB galaxies using eye magnitudes has been discussed before by de Vaucouleurs, de Vaucouleurs & Buta (1981) who found similar effects in the Fisher & Tully (1975) DDO dwarf sample. The reason appears to be a subjective compression of the surface brightness scale. Additionally, for the small angular diameter sample of Thuan & Seitzer, there is a problem with their correction from UGC to Holmberg angular diameters. For galaxies with small angular diameters, the Thuan & Seitzer diameters are too large and therefore, from their equation (4), their magnitudes are too bright.

3.2 Hydrogen mass

The H I integrals of our dwarf galaxy sample are relatively well determined. To correct the H I mass for the slight

Table 2. Derived galaxy properties.

(1) GALAXY	(2) ℓ b ($^{\circ}$)	(3) V_0 km s^{-1}	(4) D Mpc	(5) d kpc	(6) F_c f_c	(7) q i	(8) σ V_{rot} km s^{-1}	(9) $M_T(V, \sigma)$ $M_T(V)$ $\times 10^8 M_{\odot}$	(10) M_B ΔM_B mag	(11) $\log L_B$	(12) $\log M_H$	(13) $\log M_T$
0049-01	123.3 -64.5	2022	27.0	3.4	0.19 1.00	0.34 64	10 17	2.1 2.2	-15.0 -0.22	8.18	8.14	8.33
0049-00	123.2 -63.4	1735	23.1	6.7	3.74 1.00	0.27 71	28 57	42.4 50.2	-16.8 -0.22	8.88	9.30	9.63
UGC 695	131.5 -61.5	737	9.8	5.1	0.82 1.02	0.52 37	14 18	5.4 5.8	-15.1 -0.23	8.20	7.90	8.74
DDO 26	148.2 -28.0	1162	15.5	15.8	3.49 1.06	0.37 61	11 19	12.9 12.7	-16.2 -0.43	8.63	8.92	9.11
Mkn 600	170.0 -47.2	1052	14.0	3.5	1.61 1.00	0.41 56	18 27	6.7 7.0	-15.6 -0.27	8.40	8.50	8.82
UGC 2684	166.3 -32.7	408	5.4	4.4	2.05 1.04	0.35 63	15 25	6.5 6.5	-12.5 -0.37	7.18	7.78	8.81
UGC 3817	172.9 24.1	472	6.3	5.1	1.93 1.04	0.35 63	7 13	1.9 2.2	-13.7 -0.49	7.64	7.88	8.27
DDO 47	203.1 18.5	160	2.9	6.5	14.93 1.35	0.50 40	18 22	10.4 11.7	-14.4 -0.63	7.92	8.10	9.02
UGC 4483	145.0 34.4	297	4.0	2.2	2.95 1.02	0.35 63	7 11	0.7 0.9	-13.3 -0.35	7.50	7.67	7.81
UGC 4824	166.9 42.5	601	8.0	7.9	0.27 1.04	0.20 76	5 14	2.4 3.3	-15.5 -0.30	8.37	7.24	8.39
1 Zw 18	160.5 44.8	825	11.0	1.9	0.80 1.00	0.26 72	9 19	1.3 1.3	-14.3 -0.28	7.89	7.99	8.11
UGC 6248	244.3 61.3	1159	15.5	9.9	0.39 1.03	0.50 40	6 8	2.0 3.4	-15.2 -0.23	8.23	7.97	8.31
UGC 6881	238.6 75.3	536	7.1	4.6	0.77 1.02	0.31 67	16 29	8.1 8.3	-13.7 -0.21	7.63	7.60	8.91
UGC 7207	160.3 77.1	1073	14.3	17.1	1.35 1.08	0.36 62	14 23	21.8 21.6	-16.5 -0.21	8.76	8.44	9.34
UGC 7298	135.2 64.1	260	3.5	1.7	1.27 1.01	0.39 59	5 8	0.3 0.6	-12.1 -0.22	7.01	7.18	7.49
RMB 56	271.8 74.8	-314	15.0	2.3	0.45 1.00	0.51 38	21 26	5.2 6.6	-15.0 -0.21	8.18	8.00	8.72
1 Zw 36	134.1 68.1	362	4.8	2.0	1.82 1.01	0.54 31	14 16	1.8 2.0	-14.1 -0.22	7.82	7.63	8.26
UGC 7605	151.0 80.1	334	4.5	2.8	1.28 1.03	0.45 51	7 9	0.7 1.0	-13.9 -0.20	7.74	7.41	7.85
RMB 132	284.2 74.2	1184	15.0	1.7	0.33 1.00	0.45 50	19 26	3.2 3.5	-14.0 -0.21	7.78	7.87	8.51
UGC 7903	125.4 63.1	553	7.4	3.0	1.63 1.01	0.58 0	29 31	12.1 -	-13.6 -0.22	7.59	7.95	9.08
UGC 8055	305.8 66.7	520	6.9	2.8	1.77 1.01	0.50 41	23 29	8.0 10.0	-13.8 -0.22	7.69	7.93	8.90
UGC 8215	114.6 70.0	309	4.1	1.7	0.91 1.01	0.50 41	7 9	0.5 0.6	-12.4 -0.21	7.12	7.19	7.66
UGC 8276	316.6 67.8	830	11.1	4.5	0.64 1.01	0.35 63	14 24	5.8 5.8	-14.3 -0.22	7.90	7.90	8.77
Mkn 450	91.5 80.8	909	12.1	5.3	0.79 1.01	0.40 58	14 22	6.4 6.3	-16.1 -0.20	8.61	8.06	8.81
UGC 9427	354.7 55.2	1565	20.9	8.5	0.69 1.01	0.43 54	32 46	49.8 61.5	-18.2 -0.24	9.46	8.48	9.70
Mkn 429	57.7 64.4	1525	20.3	4.1	0.66 1.00	0.56 22	52 59	55.0 174.1	-17.1 -0.22	8.99	8.44	9.74
1457-00	355.8 48.1	1886	25.2	2.7	0.26 1.00	0.58 0	36 38	16.2 -	-16.6 -0.27	8.79	8.22	9.21
NGC 5811	358.9 49.9	1528	20.4	7.7	0.31 1.01	0.49 42	18 23	13.3 14.8	-17.2 -0.26	9.05	8.11	9.12
UGC 9661	359.6 49.8	1240	16.5	8.2	0.34 1.02	0.48 45	22 28	20.2 23.5	-17.1 -0.26	8.99	7.96	9.31
1501+00	358.5 48.5	1588	21.2	4.8	0.26 1.00	0.45 51	8 11	1.8 2.0	-15.6 -0.27	8.40	8.07	8.26
UGC 10669	101.6 34.7	685	9.1	5.0	0.63 1.03	0.58 0	12 13	3.6 -	-13.8 -0.35	7.67	7.72	8.56
2228-00	65.7 -46.7	1778	23.7	1.9	0.14 1.00	0.29 69	14 27	2.8 2.8	-14.4 -0.27	7.94	7.90	8.44

1992MNRAS...258...334S

Table 2 – continued

(1) GALAXY	(2) ℓ b ($^\circ$)	(3) V_0 km s $^{-1}$	(4) D Mpc	(5) d kpc	(6) F_c f_c	(7) q i	(8) σ V_{rot} km s $^{-1}$	(9) $M_T(V, \sigma)$ $M_T(V)$ $\times 10^8 M_\odot$	(10) M_B ΔM_B mag	(11) $\log L_B$	(12) $\log \dot{M}_H$	(13) $\log \dot{M}_T$
DDO 214	64.0 -49.7	1864	24.9	25.3	4.67 1.07	0.52 35	29 35	109.7 168.6	-18.6 -0.26	9.62	9.46	10.04
UGC 12151	69.0 -48.4	1945	25.9	30.9	4.72 1.09	0.44 53	35 50	214.0 273.2	-17.8 -0.27	9.30	9.50	10.33
UGC 12178	76.0 -44.6	2135	28.5	43.1	6.13 1.12	0.37 61	42 68	481.8 615.8	-19.3 -0.28	9.87	9.70	10.68
UGC 12894	112.3 -22.3	591	7.9	3.2	1.08 1.01	0.58 0	11 12	2.0 -	-13.5 -0.53	7.57	7.82	8.30

Notes. Distances assume $H_0 = 75 \text{ km s}^{-1} \text{ Mpc}^{-1}$ except for DDO 47 at 2.9 Mpc (Fisher & Tully 1975) and both RMB 56 and RMB 132 which are assumed to be members of the Virgo Cluster at 15 Mpc.

resolution of the galaxies in the Lovell telescope beam, we have assumed an H I distribution modelled as an elliptical Gaussian with a half-power major diameter equal to the Holmberg diameter and an axial ratio equal to the Holmberg axial ratio. Huchtmeier (1980) confirms this choice with a sample of 21 late-type irregular galaxies for which he finds a ratio of the H I extent at half power to the Holmberg diameter of 1.08 ± 0.23 . The beam correction factor is then given by

$$f_c = \left[1 + \left(\frac{a_H}{b_\theta} \right)^2 \right]^{1/2} \left[1 + \left(\frac{p_H a_H}{b_\theta} \right)^2 \right]^{1/2}, \quad (1)$$

where b_θ is the telescope beamwidth ($= 12 \text{ arcmin}$ for the Lovell Telescope), a_H is the Holmberg major axis diameter of the galaxy and p_H the Holmberg axial ratio. For blue compact galaxies Thuan & Martin (1981) use a ratio of the H I to optical extent at $25 \text{ mag arcsec}^{-2}$ of 2.4. Large values of H I-to-optical size appear to be common for BCGs (e.g. Brinks & Klein 1989). For our emission-line sample, however, the largest angular diameter is that of UGC 9661 which has Holmberg dimensions of $1.7 \times 1.3 \text{ arcmin}^2$ and blue dimensions at the $25 \text{ mag arcsec}^{-2}$ isophote of $1.2 \times 1.0 \text{ arcmin}^2$ (Seitzer, private communication). With the Lovell telescope beam the difference in beam correction factor between our correction and the Thuan & Martin correction corresponds to only 3 per cent of the measured flux, which is substantially lower than our total estimated flux uncertainties of 10 per cent. We therefore use the Huchtmeier correction for both the LSB galaxies and the blue compact galaxies in our sample. For the complete galaxy sample here, the beam correction factor is less than 12 per cent with the exception of DDO 47, a nearby dwarf irregular, which has a 35 per cent correction.

Although the optical properties of the LSB and BCG galaxies are very different, the integrated H I properties are not readily distinguished. For a given M_B the average hydrogen mass for the two classes lies within the intrinsic dispersion, as can be seen in Fig. 2. Thuan (1985) found a similar result. This conclusion is reinforced by Fig. 3 which plots M_H/L_B against M_B , where the scatter is reduced by binning the data for each class in groups of three.

The most striking result of the present survey is the finding that, for dwarf galaxies, the ratio of neutral hydrogen mass to luminosity increases significantly as the blue luminosity falls. Fig. 3 shows that this is a trend which extends from normal

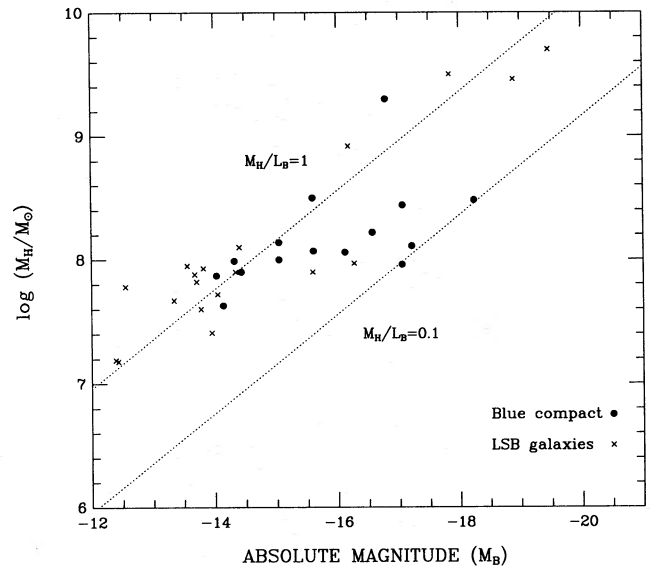


Figure 2. Neutral hydrogen mass M_H plotted against absolute blue magnitude M_B . Dotted lines show $M_H/L_B = 0.1$ and 1.0 . BCG and LSB galaxies are indicated separately.

spirals to the most dwarf H I galaxies known. The mean properties are plotted for Sbc, Sc and Scd galaxies taken from the observations by Shostak (1978) and Fisher & Tully (1981). The lowest luminosity dwarf with good H I data is the M81 group dwarf A (Sargent, Sancisi & Lo 1983) with $M_B = -11 \text{ mag}$. The best-fitting slope to the dwarf galaxies in Fig. 3 corresponds to $M_H/L_B \propto L^{-0.3 \pm 0.1}$. A similar trend for more luminous galaxies was found by Fisher & Tully (1975), and Davies & Kinman (1984) suggested that this trend extends from normal spirals to dwarf galaxies. It is interesting that Thuan & Seitzer (1979a) found no statistically significant trend for their sample of 145 UGC dwarfs. We believe that their results require a systematic correction for eye-estimates of dwarf luminosities which would be in the sense of reconciling their results with ours.

The present results also show that dwarfs with high M_H/L_B occur in the field as well as around large galaxies. The best-known H I-rich dwarf groupings are those around NGC 1023 (Davies & Kinman 1984) and M81 (Lo & Sargent 1979; Sargent *et al.* 1983).

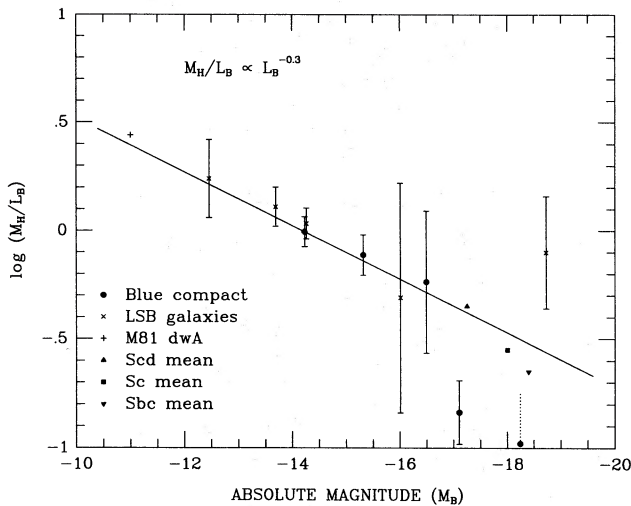


Figure 3. Neutral hydrogen mass to blue luminosity ratio plotted against absolute blue magnitude. The galaxy sample is binned into 1-mag intervals (or greater where insufficient data were available) with appropriate error bars on the mean. BCG and LSB galaxies are shown separately. Data for M81 dwarf A are from Sargent *et al.* (1983), while the Sbc, Sc and Scd galaxy averages are from Shostak (1978).

3.3 Total mass

Conventional mass estimates of spiral galaxies are based on rotationally dominated spherically symmetric models (Faber & Gallagher 1979). For normal spirals, single-dish H I observations of integrated profiles are able to reproduce masses derived from rotation curves to a close approximation (e.g. Dean & Davies 1975), but low-mass galaxies are often not straightforward disc-like systems. They almost certainly have extra support against gravitational collapse due to gas pressure, bulk velocity dispersion and stellar motions. In the case of BCGs, an increased random component can be expected due to input from supernovae and stellar winds. In the extreme case of pure velocity dispersion, some form of virial mass estimator (e.g. Volders & Högbom 1961) is appropriate.

An additional problem in the case of low-mass galaxies is that the relatively low ratio of rotation velocity to velocity dispersion means that they will have relatively thick discs. This has two consequences. The first is that our estimate of the inclination, based on the optical isophotes, will involve the use of an intrinsic axis ratio (equation 5-25b of Mihalas & Binney 1981) which is greater than the $q=0.1-0.2$ conventionally assumed for disc systems. The apparent axial ratio distribution $\phi(p)$ of dwarf irregulars, LSBs and BCGs is used in Appendix A to show that the intrinsic axial ratio distribution $\phi(q)$ is a non-single-valued distribution with a mean intrinsic axial ratio $\langle q \rangle = 0.58$. This shows that, on average, dwarf galaxies are fat, not flat objects. As discussed in Appendix A, we obtain reasonable agreement with other authors (Thuan & Seitzer 1979a; Binney & de Vaucouleurs 1981). The second consequence is that, if the total mass distribution also follows the observed (gas and stellar) mass distribution, then the inferred mass will depend, in a modest way, on the disc thickness (Schmidt 1956). Where spherical dark haloes dominate the mass distribution at the Holmberg radius, however, this is not likely to be a problem.

It can be shown from the virial theorem that a good estimator of the total mass within the Holmberg diameter a_H for a spherical isothermal galaxy is

$$\frac{M_T}{M_\odot} = 3.3 \times 10^4 a_H D (3\sigma^2 + V_{\text{rot}}^2), \quad (2)$$

where a_H is in arcmin, D is the distance in Mpc, V_{rot} is the rotation velocity (km s^{-1}) at the Holmberg radius and σ is the isotropic velocity dispersion. For a galaxy with an oblate $q=0.58$ total mass distribution, equation (2) will overestimate the mass by about 30 per cent. A Gaussian mass distribution with its total density normalized to half its central density at the Holmberg radius would lead to a value 10 per cent smaller than given in equation (2). For $\sigma=0$ this total mass estimator is mid-way between the ‘indicative mass’ estimates by Fisher & Tully (1975) and Thuan & Seitzer (1979a) on the assumption of $W_{20} = 2.4 V_{\text{rot}}$ (Fisher & Tully 1981). The decomposition of V_{rot} and σ is of course a problem for single-dish observations. We therefore adopt two standpoints in order to obtain a reasonable estimate of the range of total masses possible for a given galaxy. The first is to assume a constant value of $\sigma = 10 \text{ km s}^{-1}$, typical for spiral and dwarf galaxies (Shostak & van der Kruit 1984). The second is to estimate, for each galaxy, the most likely intrinsic axial ratio $\langle q|p \rangle$. For a given intrinsic disc axial ratio, the ratio of rotation to dispersion then follows (Binney 1978; van der Kruit & Freeman 1986), if it is assumed that any bulge component makes a negligible contribution to the apparent axial ratio for such galaxies. We use the formalism of Fall & Frenk (1983):

$$\left(\frac{V_{\text{rot}}}{\sigma}\right)^2 = \frac{(1+2q^2)\cos^{-1}q - 3q(1-q^2)^{1/2}}{q(1-q^2)^{1/2} - q^2\cos^{-1}q}. \quad (3)$$

For a given value of σ or V_{rot}/σ , we may therefore estimate V_{rot} from

$$W_{50} = 2(V_{\text{rot}} \sin i + 1.18\sigma), \quad (4)$$

which approximately describes the manner in which they combine to give the observed profile width (the 1.18 factor represents the half-power half-width of the Gaussian function). Hence, for a given linewidth W_{50} , we can solve for V_{rot} and σ using equations (3) and (4). A potentially more realistic form of equation (4) than the linear summation used is given by Tully & Fouqué (1985), but similar answers are obtained.

The mass estimates calculated for the two models are given in column 9 of Table 2. The value estimated from the deprojected shape of the galaxy and given in line 1 is used in the subsequent correlations in this paper. The value estimated from an assumed constant value (10 km s^{-1}) of σ is given in line 2. The two mass estimates are very similar by virtue of the fact that the maximum assumed value of q is 0.58 (see Appendix A). The advantage of the first estimator is that it produces a meaningful estimate even for face-on galaxies. Overall, these total mass estimates are smaller than ‘indicative mass’ estimates because the correction to the profile width for inclination is less after subtraction of the isotropic Gaussian component. This is typical for well-studied low-luminosity systems (Tully *et al.* 1978; Staveley-Smith *et al.* 1990).

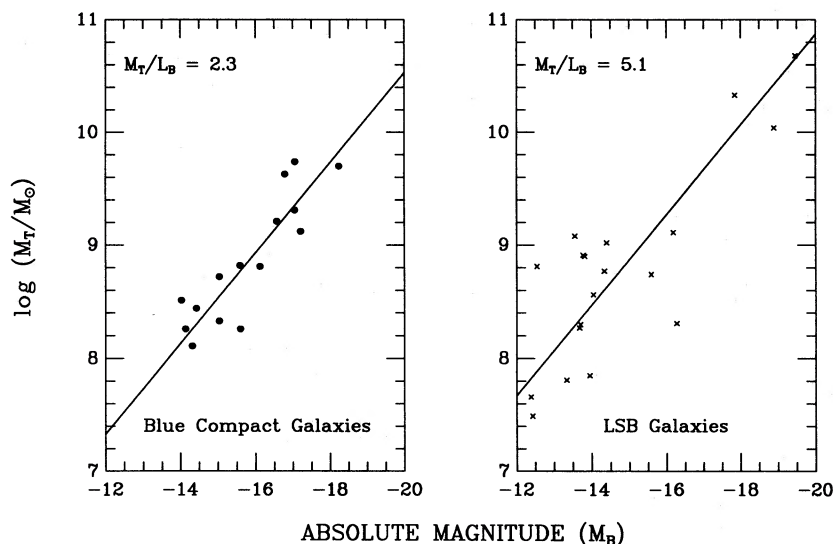


Figure 4. Total mass plotted against absolute blue magnitude for the BCG and LSB galaxies separately. Lines of constant mass-to-light ratio, $M_T/L_B = 2.3$ for BCGs and 5.1 for LSB galaxies, are shown.

Fig. 4 shows the relationship between total mass and blue luminosity for the BCGs and LSBs separately. It is evident that the M_T/L_B ratio for BCGs ($M_T/L_B = 2.3$) is significantly less than that for LSBs ($M_T/L_B = 5.1$). In the sample available, there is a smaller spread in the M_T - L_B relation for BCGs than for LSBs. A similar result for LSBs was derived by Thuan (1985), but his result for BCGs is higher than ours because he calculated M_T at $4D_{25}$. Allowing for this difference (and for the magnitude and diameter errors already mentioned), the results are in accord.

The greater mass of LSBs than BCGs for a given luminosity is approximately in proportion to their linear diameters. We should therefore emphasize that the mass estimates are made on the basis of the Holmberg diameters of these objects and not their H I diameters which are unknown in most cases. If there is significant matter beyond this diameter then M_T/L_B would be greater than the calculated values. The same holds for low-luminosity galaxies which appear to have similar values for M_T/L_B to those of brighter galaxies. If the H I-to-optical extent of these galaxies is anticorrelated with absolute luminosity (as it appears to be for such systems, e.g. DDO 154; Carignan & Beaulieu 1989), then M_T/L_B would increase with decreasing luminosity in the same way as found for M_H/L_B .

4 DISCUSSION

4.1 Dwarfs and the galaxy mass and luminosity functions

The numerical dominance of dwarf galaxies in the galaxy distribution function raises interest in the contribution of dwarf systems to the luminosity and matter content of the Universe. The data presented here lead to possible new insights.

We will use the Schechter form of the galaxy luminosity function in our calculations. It is compared with published results for dwarf galaxies in Appendix B. Since the space density diverges for a Schechter parameter $\alpha > 1$ we must introduce a lower luminosity cut-off to equation (B1). The faintest dwarf galaxies outside the Local Group with well-

determined luminosities have $M_B \sim -11$ mag (Sargent *et al.* 1983), while dwarf ellipticals can be as faint as $M_B = -8$ mag (Kraan-Korteweg & Tammann 1979). By adopting a cut-off magnitude of -10 (see Appendix B) and a value of 1.5 for α , we find the space density of galaxies to be $N = 3 \text{ Mpc}^{-3}$ and the ratio of dwarf to non-dwarf galaxies to be 40:1; the division between dwarf and non-dwarf galaxies is taken to be at $M_B = -16$ mag.

The luminosity contribution from dwarf galaxies comes mainly from the brightest dwarfs (assuming $\alpha < 2$). The ratio of the dwarf to total luminosity is 4.5 per cent for $\alpha = 1.25$ and 13 per cent for $\alpha = 1.5$.

Because of the increase of M_H/L_B with decreasing luminosity found in our galaxy sample, we expect the H I contribution of these galaxies to be correspondingly larger than their luminosity contribution. By adopting the values of $\alpha = 1.6$ and $M_H = 5.3 \times 10^9 M_\odot$ given by Fisher & Tully (1981) for brighter galaxies, we estimate that dwarf galaxies defined as having $M_H < 2 \times 10^8 M_\odot$ comprise 31 per cent of the H I mass of all galaxies. This is likely to be a lower limit, given the optically based selection criteria that even H I surveys are dependent on. Large values for the H I contribution of low-mass galaxies have important implications for the origin of the damped Ly α lines seen against QSOs (Tyson & Scalo 1988).

4.2 Starbursts in blue compact galaxies

Our data can be used to examine the hypothesis of Searle & Sargent (1972) that BCGs are LSB galaxies in a starburst phase. The properties of the two classes of galaxy may be summarized as follows.

- (i) The H I masses of BCG and LSB galaxies of a given blue luminosity are very similar (Figs 2 and 3). The velocity widths of BCGs are slightly greater for a given blue luminosity.
- (ii) The total mass within the $\mu_B = 26.5 \text{ mag arcsec}^{-2}$ isophote of a BCG is 2.2 times smaller than that of an LSB galaxy of a given blue luminosity; Fig. 4 illustrates this dif-

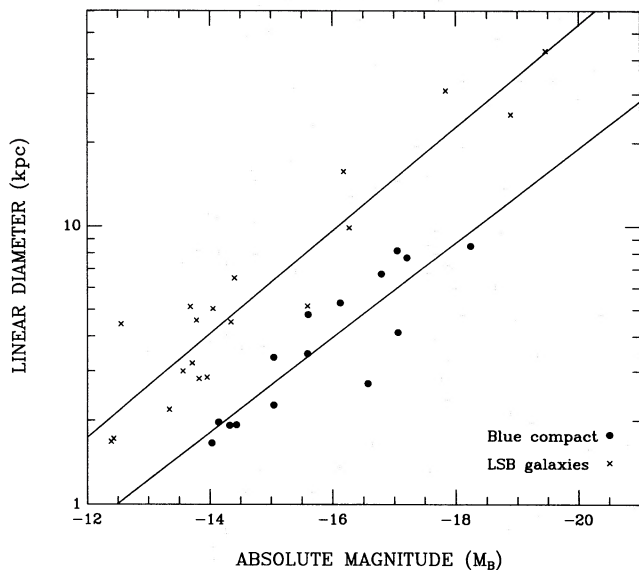


Figure 5. Linear Holmberg diameter plotted against absolute blue magnitude, with BCG and LSB galaxies shown separately. Least-squares regressions are shown for each class of galaxy. The heterogeneous diameter data imply substantial errors for individual galaxies, though these are insufficient to explain the gross difference between LSB and BCG diameters.

ference where the best-fitting values of M_T/L_B for BCG and LSB galaxies are 2.3 and 5.1 respectively.

(iii) The linear diameter of BCGs of a given blue luminosity is a factor of ~ 2.5 smaller than the corresponding LSB galaxy (Fig. 5). Both types of galaxy have the same mean luminosity–diameter regression line corresponding to $L_B \propto d_H^{2.0 \pm 0.2}$, where d_H is the Holmberg diameter.

At face value, these results appear to indicate that BCG and LSB galaxies belong to galaxy populations with different total masses and linear dimensions for a given blue luminosity. The larger total masses of the LSB galaxies are mainly the result of their larger diameters; the velocity widths of the two classes are similar.

It could, however, be argued that the observed properties (ii) and (iii) are the consequence of the BCGs being more luminous during the starburst phase, following the Searle & Sargent model. Fig. 5 and the relation in (iii) above show that the luminosity increase at a fixed diameter is a factor of 8. We would then require that the starbursts are preferentially triggered in high- M_H LSB galaxies to satisfy (i) above. Also, we would require that, having undergone a burst of star formation, the kinetic energy from young stellar winds and supernova explosions is efficiently transferred to the neutral gas. This reconciles the low velocity widths in the host LSBs compared to the higher velocity widths seen in the brighter BCGs. We estimate that for a factor of 8 brightening in the transition from LSB to BCG, the broadening for a $M_B = -16$ mag BCG would be about 30 km s^{-1} . Such broadening may take the form of an outflow or an increased dispersion. Because the velocities are close to escape velocity, an extensive halo of dark matter would be required for gas retention. There are obvious problems in dissipating this energy and returning to the quiescent phase as demanded by the oscillatory-type evolutionary model

(LSB–BSG–LSB). In particular, many LSB galaxies have well-defined, low-dispersion rotating discs which appear undisturbed (e.g. Skillman *et al.* 1987), and some, but not all, BCGs have extensive H I haloes more characteristic of large-scale rotation than outflow or dispersion (e.g. Brinks & Klein 1988). These questions are best answered by detailed H I aperture synthesis and optical imaging of these galaxies, but we consider that the present indications favour the scenario that only some, if any, LSB galaxies become BCGs, and that as a class they are probably unrelated.

5 CONCLUSIONS

We have used the integrated H I and optical properties of a sample of dwarf galaxies to compare the characteristics of blue compact galaxies and low surface brightness galaxies. Both types of galaxy are hydrogen-rich and show an increase of M_H/L_B with decreasing L_B amounting to a factor of 3 in 4 mag. The contribution of blue luminosity in dwarfs between $M_B = -16$ to -10 mag is 13 per cent of the total blue luminosity of galaxies. The H I mass of dwarfs from optically selected samples is 31 per cent of all galaxies.

The present observations of integrated properties suggest the next steps to be taken to resolve the question of the relationship between BCG and LSB galaxies. Although we conclude from the present data that the two types are unrelated, a more definitive understanding requires detailed study of individual galaxies. At the centre of the discussion is the question of the extent of an underlying LSB-type component in BCG galaxies. CCD imaging of BCGs (e.g. Loose & Thuan 1988; Kunth *et al.* 1988) showed that luminosity extends beyond the bright knots. The radial distribution and colour of this underlying stellar distribution requires comparison with that of LSB galaxies. Even more fundamental information can be derived from H I aperture synthesis observations of the two classes of dwarf galaxy. These can give the gaseous and total mass distribution within each galaxy which, on comparison with the optical data, leads to an estimate of the dark matter distribution. Only a few BCG and LSB galaxies have been mapped fully in H I. Both classes of galaxy have H I well beyond the optical extent (e.g. Viallefond & Thuan 1983; Carignan & Beaulieu 1989).

The present list of H I detections is a useful source of galaxies for further detailed high-resolution optical and H I studies.

REFERENCES

- Abell, G. O., 1977. *Astr. J.*, **213**, 327.
- Abramowitz, M. & Stegun, I. A., 1965. *Handbook of Mathematical Functions*, Dover, New York.
- Auman, J. R., Hickson, P. & Fahlman, G. G., 1982. *Publs astr. Soc. Pacif.*, **94**, 19.
- Binggeli, B., Sandage, A. & Tarenghi, M., 1984. *Astr. J.*, **89**, 64.
- Binney, J., 1978. *Mon. Not. R. astr. Soc.*, **183**, 501.
- Binney, J. & de Vaucouleurs, G., 1981. *Mon. Not. R. astr. Soc.*, **194**, 679.
- Bothun, G. D., Impey, C. D. & Malin, D. F., 1991. *Astrophys. J.*, **376**, 404.
- Brinks, E. & Klein, U., 1988. *Mon. Not. R. astr. Soc.*, **231**, 63p.
- Brinks, E. & Klein, U., 1989. *Astrophys. Space Sci.*, **156**, 183.
- Carignan, C. & Beaulieu, S., 1989. *Astrophys. J.*, **347**, 760.

- Davies, R. D. & Kinman, T. D., 1984. *Mon. Not. R. astr. Soc.*, **207**, 173.
- Dean, J. F. & Davies, R. D., 1975. *Mon. Not. R. astr. Soc.*, **170**, 503.
- de Vaucouleurs, G., de Vaucouleurs, A. & Corwin, H. G., 1976. *Second Reference Catalogue of Bright Galaxies*, University of Texas Press, Austin (RC2).
- de Vaucouleurs, G., de Vaucouleurs, A. & Buta, R., 1981. *Astr. J.*, **86**, 1429.
- De Young, D. S. & Gallagher, J. S., 1990. *Astrophys. J. Lett.*, **356**, L15.
- Faber, S. M. & Gallagher, J. S., 1979. *Ann. Rev. Astr. Astrophys.*, **17**, 135.
- Fall, S. M. & Frenk, C. S., 1983. *Astr. J.*, **88**, 1626.
- Felten, J. E., 1977. *Astr. J.*, **82**, 861.
- Fisher, J. R. & Tully, R. B., 1975. *Astr. Astrophys.*, **44**, 151.
- Fisher, J. R. & Tully, R. B., 1981. *Astrophys. J. Suppl.*, **47**, 139.
- Godwin, J. C. & Peach, J. V., 1977. *Mon. Not. R. astr. Soc.*, **181**, 323.
- Gordon, D. & Gottesman, S. T., 1981. *Astr. J.*, **86**, 161.
- Hoffman, G. L., Helou, G. & Salpeter, E. E., 1988. *Astrophys. J.*, **324**, 75.
- Holmberg, E., 1958. *Medd. Lunds astr. Obs.*, **2**, 136.
- Huchtmeier, W. K., 1980. In: *ESO/ESA Workshop on Dwarf Galaxies*, pp. 55, 65, eds Tarengi, M. & Kjar, K.
- Kinman, T. D. & Davidson, K., 1981. *Astrophys. J.*, **243**, 127.
- Kinman, T. D. & Hintzen, P., 1981. *Publ. astr. Soc. Pacif.*, **93**, 405.
- Kinman, T. D., Rubin, V. C., Thonnard, W. N., Ford, W. K. & Peterson, C. J., 1977. *Astr. J.*, **82**, 879.
- Kraan-Korteweg, R. C. & Tammann, G. A., 1979. *Astr. Nachr.*, **300**, 181.
- Kunth, D., Maurogordato, S. & Vigroux, L., 1988. *Astr. Astrophys.*, **204**, 10.
- Lang, K. R., 1974. *Astrophysical Formulae*, Springer, Berlin.
- Lo, K. Y. & Sargent, W. L. W., 1979. *Astrophys. J.*, **227**, 756.
- Longmore, A. J., Hawarden, T. G., Goss, W. M., Mebold, U. & Webster, B. L., 1982. *Mon. Not. R. astr. Soc.*, **200**, 325.
- Loose, H.-H. & Thuan, T. X., 1985. In: *Star-forming dwarf galaxies*, p. 73, eds Kunth, D., Thuan, T. X. & Van, J. T., Lee Printing, Singapore.
- Lucy, L. B., 1974. *Astr. J.*, **79**, 745.
- Mihalas, D. & Binney, J., 1981. *Galactic Astronomy*, 2nd edn, Freeman.
- Nilson, P., 1973. *Uppsala General Catalogue of Galaxies*, Royal Society of Sciences of Uppsala, Uppsala, Sweden.
- Reaves, G., 1983. *Astrophys. J. Suppl.*, **53**, 375.
- Sandage, A. & Binggeli, B., 1984. *Astr. J.*, **89**, 919.
- Sargent, W. L. W., Sancisi, R. & Lo, K. Y., 1983. *Astrophys. J.*, **265**, 711.
- Schechter, P., 1976. *Astrophys. J.*, **203**, 297.
- Schmidt, M., 1956. *Bull. astr. Inst. Neth.*, **13**, 15.
- Schneider, J. E., Thuan, T. X., Magri, C. & Wadiak, J. E., 1990. *Astrophys. J. Suppl.*, **72**, 245.
- Searle, L. & Sargent, W. L. W., 1972. *Astrophys. J.*, **173**, 25.
- Shostak, G. S., 1978. *Astr. Astrophys.*, **68**, 321.
- Shostak, G. S. & van der Kruit, P. C., 1984. *Astr. Astrophys.*, **132**, 20.
- Skillman, E. D., Bothun, G. D., Murray, M. A. & Warmels, R. H., 1987. *Astr. Astrophys.*, **185**, 61.
- Staveley-Smith, L., Bland, J., Axon, D. J., Davies, R. D. & Sharples, R. M., 1990. *Astrophys. J.*, **364**, 23.
- Tammann, G. A., 1980. In: *ESO/ESA Workshop on Dwarf Galaxies*, pp. 3, 45, eds Tarengi, M. & Khar, K.
- Thuan, T. X., 1985. *Astrophys. J.*, **299**, 881.
- Thuan, T. X. & Seitzer, P. O., 1979a. *Astrophys. J.*, **231**, 327.
- Thuan, T. X. & Seitzer, P. O., 1979b. *Astrophys. J.*, **231**, 680.
- Thuan, T. X. & Martin, G. E., 1981. *Astrophys. J.*, **247**, 823.
- Tully, R. B. & Fouqué, P., 1985. *Astrophys. J. Suppl.*, **58**, 67.
- Tully, R. B., Bottinelli, L., Fisher, J. R., Gougenheim, L., Sancisi, R.

- & van Woerden, H., 1978. *Astr. Astrophys.*, **63**, 37.
- Tyson, N. D. & Scalzo, J. M., 1988. *Astrophys. J.*, **329**, 618.
- van der Kruit, P. C. & Freeman, K. C., 1986. *Astrophys. J.*, **303**, 556.
- Viallefond, F. & Thuan, T. X., 1983. *Astrophys. J.*, **269**, 444.
- Volders, L. & Högbom, J. A., 1961. *Bull. astr. Inst. Neth.*, **15**, 307.
- Zwicky, F., 1957. *Morphological Astronomy*, p. 220, Springer-Verlag, Berlin.

APPENDIX A: THE INTRINSIC AXIAL RATIO AND INCLINATION OF DWARF GALAXIES

The intrinsic axial ratio (q) for dwarf galaxies is obtained from a consideration of the distribution in observed axial ratio (p) in large samples. We use a basic sample of 483 galaxies listed in UGC as dwarf or dwarf irregular. The observed axial ratio distribution function, $\phi(p)$, is obtained by correcting individual values to the Holmberg system by the formula of Fisher & Tully (1981):

$$p_H = 0.91 p_{\text{UGC}} + 0.09. \quad (\text{A1})$$

The resulting distribution (Fig. A1) shows a power-law increase towards higher axial ratios (lower eccentricities); it cannot be reproduced using an intrinsic distribution with a unique axial ratio.

To determine the true intrinsic distribution function we follow the method of Fall & Frenk (1983) and fit a normalized power law of the form

$$\phi(p) = (\gamma + 1)p^\gamma \quad (\text{A2})$$

to the observed data. For this UGC sample, we find $\gamma = 1.85 \pm 0.12$ (nine bins). With $\chi^2_{\text{min}} = 27.8$, the model is seen to be a poor fit to the data because of the large number of galaxies. However, many of these galaxies have diameters listed as uncertain by Nilson, and it is not clear to what extent this has affected their binning. We have also applied equation (A2) to the LSB sample of Thuan & Seitzer (1979a), a subset of the UGC sample detected in H I ($n=96$), and find $\gamma = 1.97 \pm 0.3$ (eight bins, $\chi^2_{\text{min}} = 6.5$), a good fit to the data. The true dwarf subset of this sample ($M_B \geq -16$ mag) shows no deviations from either fit about the \sqrt{n} fluctuations expected. Fitting equation (A2) to the Gordon & Gottesman (1981) sample of blue compact galaxies corrected to Holmberg axial ratios leads to $\gamma = 1.7 \pm 0.2$ (nine bins, $\chi^2_{\text{min}} = 8.0$), again a good fit to the data.

The mixed BCG and LSB sample presented here has a $\chi^2_{\text{min}} = 7.7$ (six bins) for the $\gamma = 1.85$ model, implying that there are no fluctuations from this model beyond those statistically expected.

The relationship between $\phi(p)$ and $\psi(q)$, the intrinsic axial ratio distribution function, is

$$\phi(p) = p_0 \int_0^p \frac{\psi(q) dq}{\sqrt{(1-q^2)}\sqrt{(p^2-q^2)}} \quad (\text{A3})$$

for oblate spheroids (Mihalas & Binney 1981). The solution for $\psi(q)$ in equation (A3) with $\phi(p) = 2.85 p^{1.85}$ is

$$\psi(q) = 2.716 q^{0.85} \sqrt{(1-q^2)}. \quad (\text{A4})$$

This function implies that the mean intrinsic axial ratio for dwarf galaxies is $\langle q \rangle = 0.57$, twice as large as the most commonly used values. Agreement with this value comes

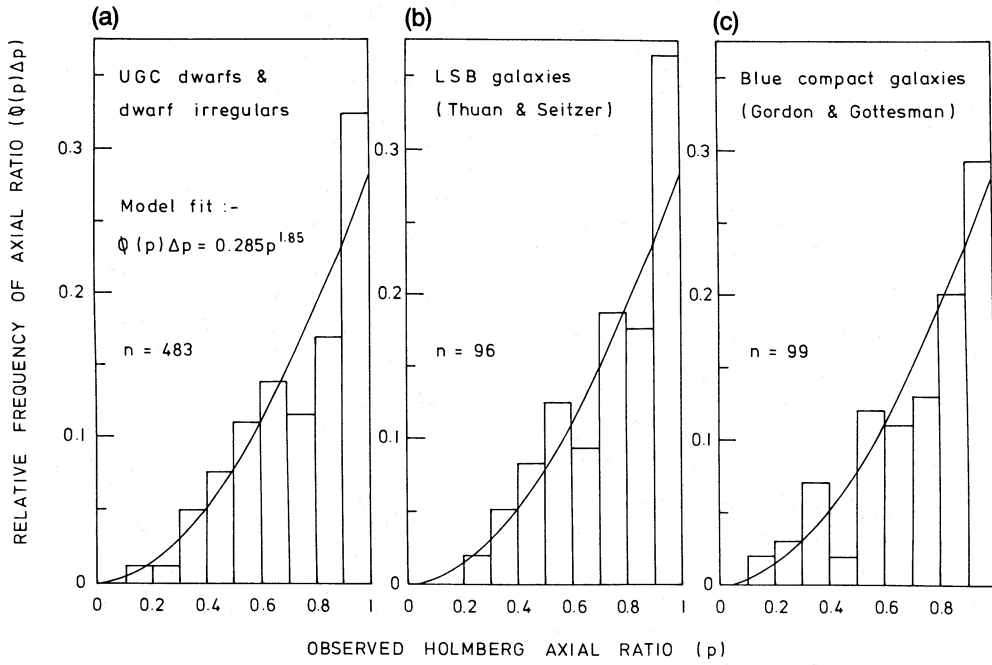


Figure A1. The relative frequency histograms of observed Holmberg axial ratios for three different galaxy samples. (a) Dwarf and dwarf irregular galaxies in the UGC; (b) UGC LSB galaxies detected in H I by Thuan & Seitzer (1979a); (c) BCGs in the list by Gordon & Gottesman (1981). The model fit by a power law with an index of 1.85 is shown in each case.

from Thuan & Seitzer (1979b), who argue that a flat intrinsic distribution from $q = 0.25$ to 1 (i.e. $\langle q \rangle = 0.625$) gives a good fit to their data. Binney & de Vaucouleurs (1981), using the inversion algorithm of Lucy (1974), have shown the intrinsic distribution of RC2 galaxies of de Vaucouleurs type $T=8$ and later to be approximately flat between 0.2 and 0.8. Again this result predicts a high mean axial ratio ($\langle q \rangle = 0.5$). A cautionary note must be added here – the shape of the function $\psi(q)$ (equation A4) is sensitive to the fitting function for $\phi(p)$ (equation A2) and we are in fact able to reduce χ^2 to 15.5 for the UGC ($n=483$) dwarfs by the use of an intrinsic distribution flat between 0.18 and 0.98 ($\langle q \rangle = 0.58$). Fortunately, it is only the cumulative form of equation (A4) that is of interest here.

Because we have a continuous distribution, there cannot be a unique solution for the intrinsic shape for a given projected shape (for $p > 0$). However, we can estimate the most likely value for q for a given projected axial ratio, p . This is

$$\langle q|p \rangle = \frac{\int_0^p q\psi(q) dq}{\int_0^p \psi(q) dq}. \quad (\text{A5})$$

An adequate approximation to equation (A5) with $\gamma = 1.85$ is

$$\langle q|p \rangle = 0.65p - 0.072p^{3.9}. \quad (\text{A6})$$

Thus the most likely inclination, i , from face-on for a galaxy of an observed axial ratio, p , can be estimated from

$$\cos^2 i = \frac{p^2 - (0.65p - 0.072p^{3.9})^2}{1 - (0.65p - 0.072p^{3.9})^2}. \quad (\text{A7})$$

APPENDIX B: DWARF GALAXIES AND THE GALAXY LUMINOSITY FUNCTION

The faint end of the galaxy luminosity function is becoming better determined from better H I observations and optical photometry of dwarf galaxies. We set down in this appendix the expressions which enable us to calculate the contribution of dwarfs to the number, luminosity and H I content of the Universe.

A useful parametrization of the galaxy luminosity function is the formula by Schechter (1976). The number of galaxies Mpc^{-3} with luminosities in the range L to $L + dL$ is given by

$$N\left(\frac{L}{L_*}\right) d\left(\frac{L}{L_*}\right) = n' \left(\frac{L}{L_*}\right)^{-\alpha} \exp\left(-\frac{L}{L_*}\right) d\left(\frac{L}{L_*}\right). \quad (\text{B1})$$

For blue luminosities, the parameters suggested by Felten (1977) are $n' = 0.01 [H_0/(75 \text{ km s}^{-1} \text{ Mpc}^{-1})] \text{ Mpc}^{-3}$, $\alpha = 1.25$ and $L_* = 2.5 \times 10^{10} L_\odot$. The space density of non-dwarf ($M_B < -16$ mag) field galaxies is then

$$N = 0.01 \int_{L_d/L_*}^{\infty} \left(\frac{L}{L_*}\right)^{-1.25} \exp\left(-\frac{L}{L_*}\right) d\left(\frac{L}{L_*}\right), \quad (\text{B2})$$

where $L_d = 3.6 \times 10^8 L_\odot$ is the blue luminosity corresponding to the dwarf galaxy limit of $M_B = -16$ mag. The solution is

$$N = 0.01 \Gamma(-0.25, 0.0144) \text{ Mpc}^{-3}, \quad (\text{B3})$$

where $\Gamma(a, x)$ is an incomplete gamma function (Abramowitz & Stegun 1965). This gives

$$N \approx 0.07 \text{ galaxies Mpc}^{-3}. \quad (\text{B4})$$

For dwarf galaxies, Holmberg examined faint companions

(mainly dEs) of Shapley-Ames galaxies. Thuan & Seitzer (1979a,b) undertook an H I survey of Nilson UGC dwarfs (mainly LSB) not already observed by Fisher & Tully (1975). Both studies indicate a luminosity function of the form

$$\log_{10} N(M_B) = 0.2 M_B + \text{constant.} \quad (\text{B5})$$

For luminosities $L \ll L^*$, the Schechter parameter, α , implied by equation (B5) is 1.5 rather than 1.25. This has interesting implications for the luminosity density of dwarf galaxies, as this diverges at $\alpha = 2$.

Further support for a luminosity function close to the form of (B5) comes from Bothun, Impey & Malin (1991), Abell (1977), Godwin & Peach (1977), Zwicky (1957), and observations by Reaves & Sandage cited in Tammann (1980), of Virgo Cluster dE galaxies. Against this, Tammann (1980) uses counts of companions of M81/Local Group to suggest that the luminosity function of spiral/Im galaxies is Gaussian. Although his result may represent the absolute magnitude distribution of such galaxies in small groups, it should not be confused with an absolute luminosity function for all galaxies. Present evidence, as Tammann himself suggests, implies that dim galaxies are preferentially found in the 'field' rather than as companions of giant galaxies.

Using equation (B1) it is straightforward to examine the contribution of dwarf galaxies to the mass, luminosity and space density of galaxies. For any Schechter parameter $\alpha > 1$ the density of dwarf galaxies diverges, so we must introduce a lower luminosity cut-off to equation (B1) corresponding to a point below which we either observe no galaxies or at least cease to call them galaxies. The faintest dwarf irregular with a reliable magnitude so far observed is M81dwA at $M_{\text{pg}} = -11.0$ mag (Sargent *et al.* 1983) and the faintest dwarf elliptical is DDO 208 at $M_B = 0.8$ mag (Kraan-Korteweg & Tammann 1979).

If the cut-off luminosity is L_c , then we reach a space density $N = 50 \text{ Mpc}^{-3}$ at $M_B = -4$ mag. There is no obser-

vational basis for a galaxy luminosity function to reach such low luminosities. The only observational limit we can derive from our work is the ill-defined magnitude where $M_{\text{H}} \approx 0.75 M_{\text{T}}$ within the Holmberg diameter, the point at which there are no stars (or dark matter), only neutral hydrogen and helium. Using the average M_{T}/L_B of LSB galaxies of 5.1, and extrapolating Fig. 3 to the point at which the above condition is met, then they will cease to have stars at $M_B \approx -9.5$ mag. If we conservatively use a cut-off magnitude of -10 mag and $\alpha = 1.5$, we find that the space density of galaxies is $N = 3 \text{ Mpc}^{-3}$, or a ratio of dwarf to non-dwarf galaxies of 40:1.

For $\alpha < 2$, the main luminosity contribution from the dwarf galaxies comes from the brightest dwarfs, and we calculate the ratio of dwarf galaxy to total galaxy luminosity as

$$L_{\text{D}}/L_{\text{TOT}} = (L_{\text{d}}/L^*)^{2-\alpha} \gamma^*(2-\alpha, L_{\text{d}}/L^*), \quad (\text{B6})$$

where $\gamma^*(a, b)$ is another incomplete gamma function, which gives the ratio $L_{\text{D}}/L_{\text{TOT}} = 4.5$ per cent for $\alpha = 1.25$ and 13 per cent for $\alpha = 1.5$.

Because of the increase in M_{H}/L_B found in our galaxy sample for lower luminosity systems, we may expect the H I contribution of these galaxies to be correspondingly larger than their luminosity contribution. In fact, by fitting a Schechter-type luminosity function to their sample of 1171 galaxies detected in H I, Fisher & Tully (1981) have deduced the H I Schechter parameters $\alpha_{\text{H}} = 1.6$ and $M_{\text{H}}^* = 5.3 \times 10^9 M_{\odot}$. The contribution of dwarf galaxies to the total H I is therefore

$$\frac{M_{\text{H}}(\text{dwarf})}{M_{\text{H}}(\text{total})} = \left(\frac{2 \times 10^8}{5.3 \times 10^9} \right)^{0.4} \gamma^* \left(0.4, \frac{2 \times 10^8}{5.3 \times 10^9} \right), \quad (\text{B7})$$

where we have defined a dwarf galaxy as having an H I mass of less than $2 \times 10^8 M_{\odot}$. This implies a substantial H I contribution of ~ 31 per cent to the total H I density.